Experimental Investigation Of Multiple-Loaded Diagonal Conducting Wall Generators

Author(s): J. W. Muehlhauser, Tran My, M. H. Scott, Y. C. L. Wu, and J. B. Dicks

Session Name: Combustion Gas MHD Generators

SEAM: 16 (1977)

SEAM EDX URL: https://edx.netl.doe.gov/dataset/seam-16

EDX Paper ID: 666

EXPERIMENTAL INVESTIGATION OF MULTIPLE-LOADED DIAGONAL CONDUCTING WALL GENERATORS*

BY

J. W. Muehlhauser, Tran My, M. H. Scott, Y.C.L. Wu
and J. B. Dicks

Energy Conversion Division
The University of Tennessee Space Institute
Tullahoma, Tennessee 37388

Abstract

Two multiple-loading schemes were investigated with a 60° diagonal conducting wall generator. Analysis has shown that the feed-back coupling scheme, where a common current return path is used, requires $I_{g_1} > I_{g_2} > \cdots > I_{g_n}$, where I_{g_j} is the generator current flowing between the (j-1)th and jth loads. Disruption of this pattern implies "energy-sink mode" operation at that location. The direct-coupling mode operated favorably as a loading scheme. Changing the load at one section does not effect the operation of other parts of the generator.

Large voltage fluctuations were observed near the exit of the generator. This fluctuation is caused by severe inter-electrode current leakage rather than instabilities. High frequency data were obtained which showed a large difference in behavior at the downstream portion of the generator.

Preliminary results were obtained on current distribution on the collection electrodes. Currents are non-uniform, however loading schemes have no significant effect. The specific distribution seems to be more combustor related than electrically related.

I. Introduction

The flexibility of the loading scheme on diagonal conducting wall (DCW) generator, as shown schematically in Fig. 1, permits one to load the generator in either a single load (two-terminal mode), or multiple level configuration. The choice of loading scheme depends primarily on the interaction parameter of the generator. For small generators, the plasma properties and consequently, the duct cross-sectional area, do not vary appreciably along the channel. The internal impedance for each electrode-volume remains fairly uniform along the generator and, therefore, a single load is adequate. However, for a large generator, as will be encountered in central power plant application, the situation will be to the contrary. The impedance match becomes very critical for optimizing the power output of the generator.

To elaborate on this point further, let us consider the short circuit current I_s of a DCW generator[1],

$$I_s = \sigma AUB(1-\Delta_s)\frac{\Omega+\phi}{1+\Omega^2}$$

where σ is electrical conductivity, A the cross-sectional area, U the velocity, B the magnetic induction strength, Ω the Hall parameter, ϕ is the direction of the electric field (ϕ=0 for Hall generator), and Δ_s is the dimensionless effective voltage drop. The short circuit currents corresponding to the entrance and exit regions can be approximated by

$$\frac{I_{s_1}}{I_{s_2}} \approx \frac{A_1}{A_2}\frac{\sigma_1}{\sigma_2}\frac{\Omega_1+\phi_1}{\Omega_2+\phi_2}\frac{1+\Omega_2^2}{1+\Omega_1}$$

where subscripts 1 and 2 refer to the entrance and exit conditions, respectively. For typical central power plant conditions, we may have

$$\frac{A_1}{A_2} \approx \frac{1}{5}, \quad \frac{\sigma_1}{\sigma_2} \approx 4, \text{ and } \frac{\Omega_1}{\Omega_2} \approx \frac{1}{4}.$$

The corresponding short circuit currents ratio becomes

$$\frac{I_{s_1}}{I_{s_2}} \approx 2.72 \text{ for constant } 45^\circ \text{ angle}$$

$$\approx 3.24 \text{ for constant } 30^\circ \text{ angle}$$

$$\approx 4.45 \text{ for } 30^\circ \text{ angle at the upstream and } 20^\circ \text{ angle at the downstream.}$$

The generator length to mean diameter ratio remains nearly constant for all sizes of generators due to pressure and friction losses along the channel. However, the generator impedance varies as the length to area ratio. Therefore, as the generator size increases, its impedance decreases, almost inversely proportional to the generator diameter (or its equivalent). One therefore expects to operate a large generator at loads (1 ohm or less). The above values of the short circuit currents ratio indicate that the generator cannot carry the same amount of load current efficiently throughout the entire generator length. If the current is higher than the generator can produce at any given location, this section will then "absorb" power from other sections and operate in the "energy sink" mode.[2] On the other hand, if the load current is too low, in addition to the mis-matched impedance, an undesirable high Hall voltage will be generated. For commercial MHD power plants, the control of the generator is extremely important. Multiple-loading offers the means for such control as compared to the single load configuration.

II. Analysis

Two limiting multiple-load schemes are considered here. One scheme offers maximum interaction among the different loads, while the other decouples the various loads. Other loading schemes can be considered as intermediate situations. For example the multiple-load schemes used in the dia-

*Work supported by ERDA under Contract No. EX-76-C-01-1760

gonal conducting wall channels at the U-25 facility[3,4] is an intermediate loading scheme. Preliminary results[5] were reported previously of the two loading schemes. One loading scheme has a common terminal at the entrance of the generator as shown on Fig. 2 along with its equivalent circuit. This scheme (feed-back coupling) was used in the ECAS studies[6]. The other scheme essentially divides the generator into a number of sub-generators as shown in Fig. 3. Each section operates very much like a single-load generator.

At weak to moderate interactions, the load line of a generator is linear. Therefore, two parameters can determine the characteristics of the generator. In the equivalent circuits as shown in Figs. 2(b) and 3(b), the open circuit voltage, V_o, and internal resistance, R_i, are chosen as the two parameters.

1. Direct-Coupling Scheme

As shown in Fig. 3, the generator is subdivided into n sections. Each sub-generator resembles a single-load generator. The generator current I_g and load current I_L are identical. Let V_{o_j}, I_{g_j}, R_{L_j}, R_{i_j} be the open circuit voltage, generator current, load and impedance of section j. $I_{j,j+1}$ is the current flowing between sub-generators j and j+1. It is clear that when $I_{j,j+1} = 0$ for j = 1, n-1, the multiple-load reduces to the single load case.

From the equivalent circuit, Fig. 3(b), the generator currents can be written in terms of the open circuit voltage, internal impedance and the load as

$$I_j = \frac{1}{R_{L_j} + R_{L_j}} V_{o_j} \quad , j=1,2, \ldots, n \tag{1}$$

Theoretically, the maximum power output that can be transfered to the external loads is

$$P_{max} = \frac{1}{4} \sum_{j=1}^{n} \frac{V_{o_j}^2}{R_{i_j}} \tag{2}$$

2. Feedback Coupling Scheme

This loading scheme as shown in Fig. 2 is characterized as feedback loading since several feedback paths are provided for the generator current. All loads are connected electrically to different sections of the generator and have a common return path. The characteristics of each section depends on the rest of the generator, hence provide maximum interaction. The generator currents can be derived from the equivalent circuit in terms of the open circuit voltage, internal impedance and the load by using the mesh-equation as

(3)

$$\begin{bmatrix} V_{o_1} \\ V_{o_2} \\ \cdot \\ \cdot \\ V_{o_n} \end{bmatrix} = \begin{bmatrix} (R_{i_1} + R_{L_1}) & (-R_{L_1}) & \cdots & 0 \\ (-R_{L_1}) & (R_{i_2} + R_{L_1} + R_{L_2}) & \cdots & 0 \\ \cdot & \cdot & \cdots & \cdot \\ \cdot & \cdot & \cdots & \cdot \\ 0 & 0 & \cdots & (-R_{L_{n-1}})(R_{i_n} + R_{L_{n-1}} + R_{L_n}) \end{bmatrix} \begin{bmatrix} I_{g_1} \\ I_{g_2} \\ \cdot \\ \cdot \\ I_{g_n} \end{bmatrix}$$

The generator current in any section may be obtained by solving equation (3).

The power output of the generator is simply

$$P = R_{L_1} I_{L_1}^2 + R_{L_2} I_{L_2}^2 + \ldots R_{L_n} I_{L_n}^2 \tag{4}$$

Rearranging equation (3), we can write the external load as following:

$$R_{L_1} = \frac{V_{o_1} - R_{i_1} I_{g_1}}{I_{L_1}}$$

$$R_{L_n} = \frac{(V_{o_1} + V_{o_2}) - (R_{i_1} I_{g_1} + R_{i_2} I_{g_2})}{I_{L_2}} \tag{5}$$

$$R_{L_n} = \frac{(V_{o_1} + V_{o_2} + \ldots + V_{o_n}) - (R_{i_1} I_{g_1} + \ldots + R_{i_n} I_{g_n})}{I_{L_n}}$$

For each generator section to operate in the generator mode[1], it is necessary that the resistive loss is less than the open circuit voltage. This means that for all sections we must have

$$(V_{o_1} + \ldots V_{o_j}) > (R_{i_1} I_{g_1} + \ldots R_{i_j} I_{g_j}) \tag{6}$$

Since the load is always positive, equation (6) requires that

$$I_{L_j} > 0 \quad , j = 1, \ldots, n \tag{7}$$

Equation (7) implies that for each generator section to operate in the generator mode, we must have

$$I_{g_1} > I_{g_2} > \ldots > I_{g_n} \tag{8}$$

since

$$\begin{aligned} I_{g_n} &= I_{L_n}, \quad I_{g_{n-1}} = I_{L_n} + I_{L_{n-1}} \\ &\cdots\cdots\cdots\cdots \\ I_{g_1} &= I_{L_n} + I_{L_{n-1}} + \ldots + I_{L_1} \end{aligned} \tag{9}$$

On the other hand, if equation (6) is not satisfied everywhere, say the jth section, then the resistive loss of the jth section is greater than open circuit voltage. In this case the generator operates in the energy-sink mode[1] where energy is supplied to the jth section by other parts of the generator. Again since the load is positive, we must have

$$I_{L_j} < 0 \tag{10}$$

consequently

$$I_{g_j} < I_{g_{j+1}} \tag{11}$$

Equation (8) implies that for each generator section to operate in the generator mode, the generator current in each section must decrease sequentially. If this pattern is destroyed at a section, that section will operate in the energy-sink mode. The limit of the energy-sink mode is

$$I_{L_j} = 0 \tag{12}$$

When the jth section operates as short circuit, thus

$$I_{g_j} = I_{g_{j+1}} \tag{13}$$

The condition imposed by equation (8) is quite restrictive. This condition is more detrimental if the load is also used as a means for control of the generator when large variation of load may be necessary.

III. Experimental Results

Both single load and multiple-load configurations were investigated. In the two multiple-load schemes discussed in the previous section, the generator was loaded in four sections (n=4). The generator contains 70 window-frame electrodes. A description of the facility and the generator can be found in Ref. 7. The first four and last four electrodes of the generator were shorted together as collecting electrodes for the end connections. In addition, electrodes (18, 19), (34, 35) and (48, 49) were used for collecting electrodes for the intermediate loads. The total mass flow was approximately 1.45 kg/sec and combustor pressure was 4 atm (absolute). The generator operated supersonically throughout the entire duct.

1. Direct Coupling Results

Figure 4 shows the Hall voltage distribution along the generator for both a 16 ohm single load and a direct-coupling multiple-load of (4, 4, 4, 4) ohms. The Hall voltage is reasonably linear except toward the downstream portion of the channel. The two different loading schemes generated comparable power (34.6 kw for single load and 35.6 kw for multiple load). However, the (2, 2, 8, 4) ohm combination (Fig. 5) produced much less power (24.5 kw) with the same total load. The reasons for the large difference in the (2, 2, 8, 4) ohm load and the small difference in the (4, 4, 4, 4) ohm load, compared with the single load, can be easily explained as follows. As reported in Ref. 5, the generator impedance per electrode was nearly constant throughout the channel. Consequently, the single load and the uniformly distributed multiple load gave the best performance. On the other hand, when the impedance is not matched, large degradation of the generator performance can be expected as was shown here.

Two multiple load distributions are shown on Fig. 5, (2, 2, 8, 4) and (2, 2, 4, 4). The Hall voltage distribution in the first two sections (2 ohm each) are nearly identical for the two configurations shown. Higher voltage was generated in the third section (8 ohm) of the first configuration compared with the third section (4 ohm) of the second configuration. In the fourth section, the two configurations again have the same load (4 ohm). The two Hall voltages become parallel to each other. This indicates that changing a load in one section does not effect the operation of other sections in the direct coupling load scheme. This result is expected for weak to moderate interactions and/or for small load changes.

2. Feed-back Coupling Results

Due to insulator deterioration, only limited results were obtained for this loading scheme. Fig. 6 shows the Hall voltage distribution for two loading distributions. For the purpose of comparison, the single load Hall voltage distribution is also shown. The entrance region operates in the energy-sink mode. From the analysis presented in the last section, we would expect that this is due to the disruption of the decreasing generator current pattern required for the generator mode operation, that is

$$I_{g_1} < I_{g_2} > I_{g_3} > I_{g_4}$$

This is indeed the case. For the two load configurations, the generator currents are (67.4, 70.7, 54.8, 40.2 amperes) and (76.3, 78.5, 60.1, 44.0 amperes), respectively.

Because only very limited results were obtained in this loading scheme, no definite conclusions can be drawn. Nevertheless the decreasing generator current criteria poses strong constraints on the generator resistance along the duct.

3. Inter-electrode Voltage Fluctuation

Large inter-electrode voltage fluctuations were observed toward the downstream portion of the generator as shown in Figs. 4 and 5. These fluctuations are associated from deterioration of the insulator. It is suspected that current leakage occurred there. It is important to notice that there is no definite frequency associated with these fluctuations. This is in contrast to the instability results of Lowenstein and Solbes[8]. Furthermore, the large fluctuations are not observed in the first three fourths of the channel. However, we expect that prolonged operation of the generator would destroy the other insulators and eventually large voltage fluctuations would exist throughout the entire generator as observed in the AVCO Mark VI channel.[9]

At the downstream portion of the generator, the Hall parameter is high resulting from lower pressure, and nonuniformities are large due to thicker boundary layers. These are the favorable conditions which promote breakdown as shown by Oliver[10]. Consequently the insulators are under more strenuous conditions in the downstream area and fail first. The large Hall voltage fluctuations near the downstream portion of the generator are the onset of the progressive deteriorations of the insulators. Better insulator material and design is the most pressing problem for long duration generator operation.

4. Current Distribution on Collecting Electrodes

Four electrodes on each end of the generator are shorted together as collecting electrodes. Figs. 7 and 8 show the current distributions for both single and multiple load configurations. The current distributions are highly nonuniform. The type of loading does not seem to significantly effect the distribution. Figs. 7 and 8 do not show any similarity at all. However a definite pattern is followed for each of the figures. This definite pattern may be combustor related. In Fig. 7, both an upstream and downstream conical combustor pieces were used in conjunction with the cylindrical main combustor. Only a downstream conical piece was used for Fig. 8. This combustor configuration is not desirable since a large portion of the generator operated in the energy sink mode as shown in Fig. 6. The poor performance is likely due to lower electrical conductivity and higher nonuniformities resulting from poor mixing and possible large eddies.

5. Fluctuations in Electrical Parameters

The experimental program includes the acquisition and analysis of data proportation to fluctuations in electrical parameters in the generator up to a frequency of 37.5 kilohertz as well as their conventional mean values. This data is

used to study the dynamics of the MHD process and to provide information concerning the interactions between parameters in the generator. A maximum of fourteen parameters can be studied for any given run.

The fluctuations in the differential voltages in a DCW generaor with a single external load are influenced by three factors; electrode surface effects, non-uniformities in the combustion plasma, and the interaction between the plasma non-uniformities and the MHD process.[11,12] The initial multiple load tests indicate that no drastic change in the basic characteristics of these fluctuations occur for multiple load as compared to the single load case. There are, however, observations worthy of mention.

The important characteristics of fluctuating data are obtained by appeal to random process theory. The fluctuation data for the multiple load tests are analyzed in terms of probabilities functions, correlation function, power spectral density functions as defined by Parzen.[13]

First, the magnitude of the fluctuations with respect to the average values is discussed. It was found that the fluctuation intensity of load current defined by the ratio of the rms to mean value,

$$\gamma_I = \frac{\sqrt{\langle I^2\rangle - \langle I\rangle^2}}{\langle I\rangle},$$

increases as the mean value decreases. The presence of large non-uniformities in the plasma effectively reduces the conductivity and the power generated is therefore reduced. The fluctuation intensity behavior is illustrated in Fig. 9 for a generator load current. A similar characteristic is observed for voltages in the generator.

For the multiple load tests, there were four collection electrodes at the ends of the generator but at points within the generator only two electrodes were used. The frequency distribution of the fluctuations for two load currents is shown in Fig. 10; one is an end current, I_E, and the other is a center current, I_D. There is a striking difference between these two functions. The current collected at two electrodes has a much higher frequency content than does the end current collected at four electrodes. The implication here is that there is a strong dependence on electrode surface effects. The low frequency behavior of the end current I_E is shown in Fig. 11. The spectral density below 100 to 200 hertz is much the same for both the two-electrode and four-electrode current collection.

The correlation functions and spectral densities of voltages in the generator are not drastically different than have been observed previously. No large changes in behavior were observed as a result of using the multiple loads rather than a single load. However, more data is necessary before firm conclusions can be drawn. The spectral densities of a differential voltage, the voltage between electrodes 26 and 27, for both loading schemes is shown in Fig. 12. The differences observed are a function of combustor performance and leakage effects.

In the case of feed-back coupled load, there were large combustion fluctuations evident in the very low frequency range (<100 hertz) of the spectral density function of this voltage. There was also excessive leakage evidenced by the large contribution in the range about 1 kilohertz. The second spectral density shown in this figure, for the direct coupled mode, is more characteristic of reasonable plasma uniformity conditions as well as adequate insulation between electrodes.

IV. Conclusions

The two loading schemes that are investigated here can be considered as two limiting cases. The feed-back coupling provides the maximum interaction among the different loading sections. Whereas the direct-coupling scheme is the minimum interacting scheme. In fact, in the direct coupling method, each loading section operates very much like an independent sub-generator. Changing load in one section does not effect the operation of the other sections as shown in Fig. 5. If the load is also used as a control device, the decoupling of the load in each section may be the most important feature. All other types of loading, for diagonal conducting wall generators, can be considered as variations of these two limiting cases.

The limited results obtained in the feed-back coupling scheme makes it difficult to draw definite conclusions. Nevertheless one would expect this scheme to be difficult to apply because all of the load sections are interacting.

Large fluctuations in Hall voltage toward the downstream end of the generator is related to the insulator deterioration rather than instability resulting from arc mode emission.[8] Consequently, the insulator is the most serious problem in limiting prolonged operation of the generator.

The current distribution on the collection electrodes does not depend on the loading schemes. However, the specific distribution may be strongly influenced by the non-uniformities of the combustion gases. Therefore the fluid mechanics aspect of the combustor operation may be more important than expected.

Analysis of high frequency fluctuations in electrical parameters have shown little difference between single load and multiple load scheme.

Acknowledgement

The authors gratefully acknowledge the excellent support of the technical staff of the Energy Conversion Division. Special thanks are due to Messers. George Charboneau, Larry Seely, and Nick Munn.

References

1. Wu, Y.C.L., "Performance Theory of Diagonal Conducting Wall MHD Generators", AIAA Journal, Vol. 14, No. 10, 1362 Oct. 1976.

2. Wu, Y.C.L., Dicks, J. B., Denzel, D. L., Witkowski, S., Shanklin, R. V., Zitzow, U., Chang, P., and Jett, E. S., "MHD Generator in Two-Terminal Operation," AIAA Journal, Vol. 6, No. 9, 1651, Sept. 1968.

3. Pischikov, S. I., and Pinkhasik, M. S., "Some Results of Investigation on the U-25 Installation", Vol. I, Proc. of the 6th Int. Conf. on MHD Electrical Power Generation, Wash. D.C., June 1975.

4. Sheindlin, A.E.; Barshak, A.E.; Bityurin, V.A.; Kovbasiuk, V.I.; Maksimenko, V.I.; Medin, S.A.; Pinkhasik, D.S.; Pishchikov and Pashkov, S.A.; "Investigation of Diagonal-Conducting-Wall R

Channel of MHD Generator of U-25 Power Plant", Proc. 15th Symp. on Engineering Aspect os MHD, Univ. Pa., Phil., Pa. May 1976.

5. Wu, Y.C.L.; Dicks, J.B.; Muehlhauser, J.W.; Scott, M.H.; Kroeger, G.; and My, Tran, "Experimental Investigation On A Direct Coal-Fired MHD Generator", ibid.

6. Seikel, G.R.; and Harris, L.P.; "A Summary of the ECAS MHD Power Plant Results", NASA TMX-73491, 1976.

7. Wu, Y.D.L; Dicks, J.B.; Tempelmeyer, K.E.; Crawford, L.W.; Muehlhauser, J.W.; Rajagopal, G. "Experimental and Theoretical Investigation on a Direct Coal Fired MHD Generator", Vol I, Proc. of the 6th Int. Conf. on MHD Electrical Power Generation, Wash. D.C., June 1975.

8. Lowenstein, A.; and Solbes, "Electrical Non-Uniformities and Their Control in Linear MHD Channels", Proc. of the 15th Symp. on Engineering Aspects of MHD, Univ. of Pa., Phil., Pa. May 1976.

9. Petty, S.; Solbes, A; Enos,G. and Dunton, A., "Progress on the Mark VI Long-Duration MHD Generator", ibid.

10. Oliver, D. A., "Inter-Electrode Breakdown on Electrode Walls Parallel and Inclined to the Magnetic Field", Vol. I, Proc. of the 6th Int. Conf. on MHD Electrical Power Generation, Wash. D.C., June 1975.

11. Scott, M. H.; Kornstett, K. and Barnett, L. "Diagnostic Instrumentation in Direct Coal-Fired MHD", Proc of the 14th Symp. on Engr. Aspects of MHD, The Univ. of Tenn. Space Inst., Tullahoma, Tenn., April 8-10, 1974.

12. Scott, M. H.; "An Experimental Investigation of Fluctuations in a Direct Coal-Fired Open Cycle MHD Generator and a Method for Modeling These Fluctuations", AIAA Paper No. 76-313,1976.

13. Parzen, Emanuel; Stochastic Processes, San Francisco: Holden-Day, 1962.

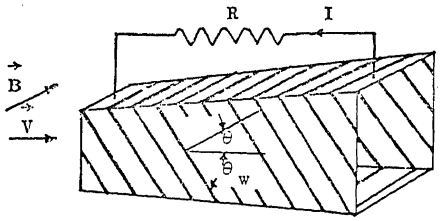

Figure 1. Schematic of Diagonal Conducting Wall (DCW) Generator Channel, Ey/Ex = tan θ = ϕ

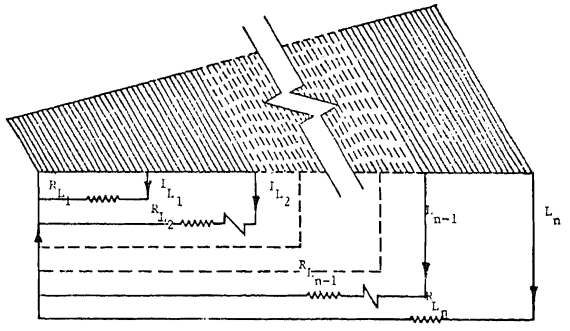

(a) Loading Schematic

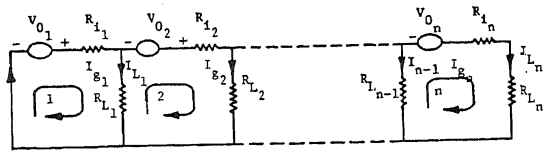

(b) Equivalent Circuit

Figure 2. Schematic Diagram of a DCW Generator with Multiple-Load Feedback Coupling and Its Equivalent Circuit

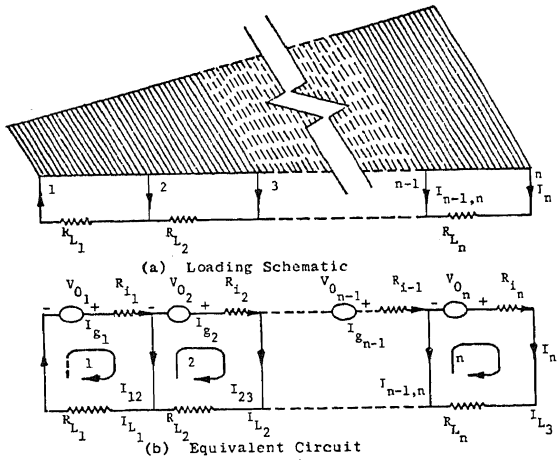

(a) Loading Schematic

(b) Equivalent Circuit

Figure 3. Direct-Coupling Loading Scheme and Its Equivalent Circuit

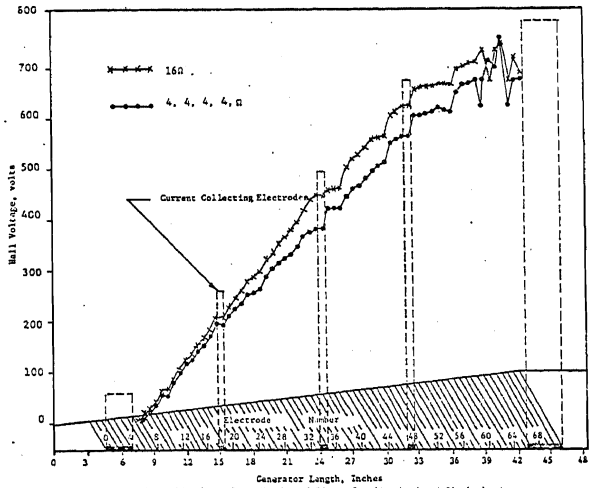

Figure 4. Hall Voltage Distribution of Direct-Coupling Load and Single Load

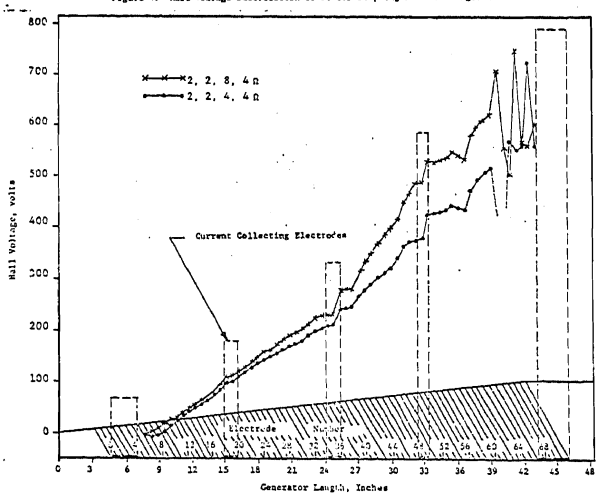

Figure 5. Hall Voltage Distribution of Direct-Coupling Load

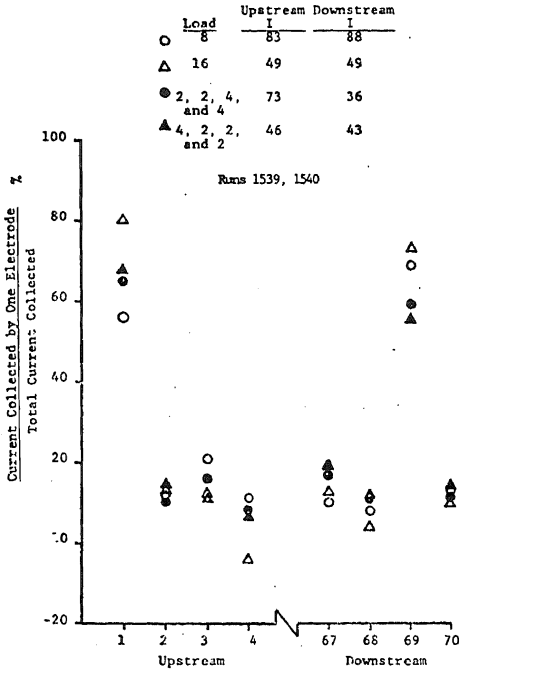

Figure 7. Current Distribution on Collection Electrodes (Single load and direct coupling load)

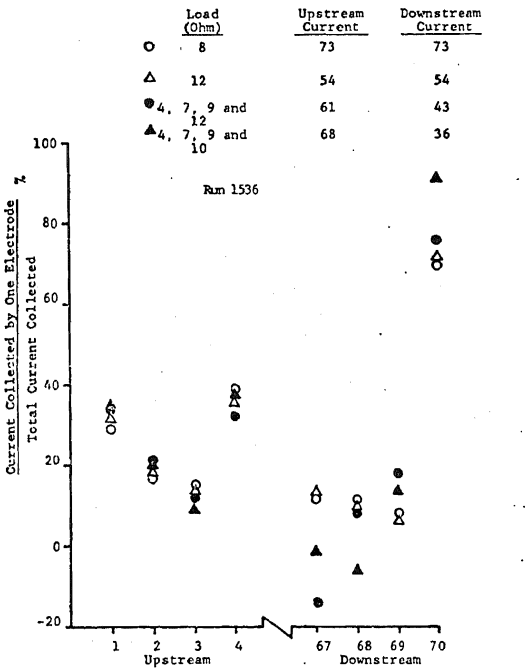

Figure 8. Current Distribution of Collecting Electrodes (Single load and feed-back coupling load)

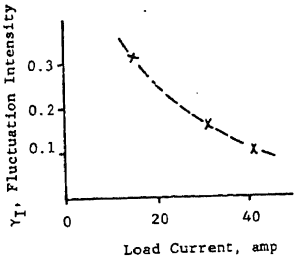

Figure 9. Fluctuation Intensity of Load Current vs. Load Current.

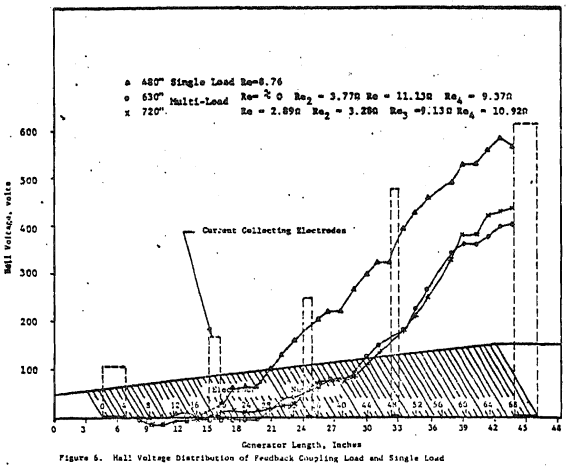

Figure 6. Hall Voltage Distribution of Feedback Coupling Load and Single Load

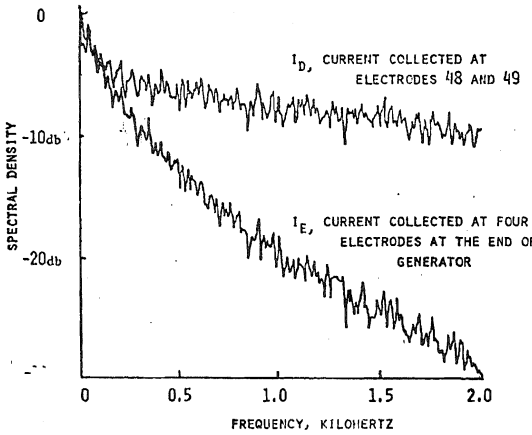

FIGURE 10. SPECTRAL DENSITY OF THE LOAD CURRENT FROM TWO COLLECTION ELECTRODES AND FROM FOUR COLLECTION ELECTRODES.

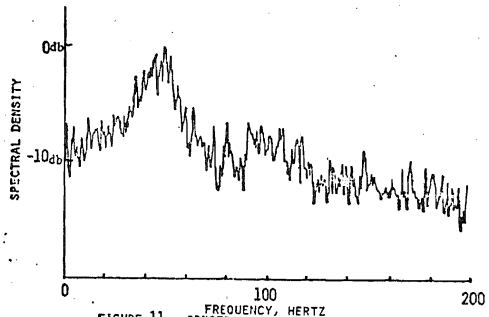

FIGURE 11. SPECTRAL DENSITY OF LOAD CURRENT, I_E, AT LOW FREQUENCY.

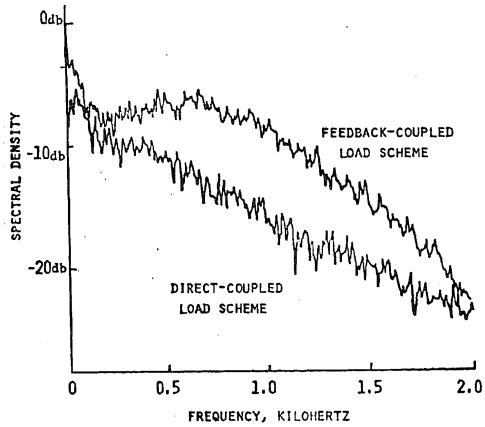

FIGURE 12. SPECTRAL DENSITY OF THE VOLTAGE BETWEEN ELECTRODES 26 AND 27 FOR BOTH MULTIPLE LOAD SCHEMES.